Modeling hypersonic boundary-layer flows with second-moment closure

By P. G. Huang

This report presents an ongoing research effort designed to apply the best possible second-moment-closure model to simulate complex hypersonic flows. The baseline model under consideration is the Launder-Reece-Rodi Reynolds stress transport turbulence model. Two add-ons accounting for wall effects are tested, namely, the Launder-Shima low-Reynolds-number model and the compressible wall-function technique. Results are reported for flow over a flat plate, both adiabatic-wall and cooled-wall cases. It has been found that further improvements of the existing models are necessary to achieve accurate prediction in high Mach number flow range.

1. Motivation and objectives

It has been reported that Reynolds-stress models yield marked improvements in predicting a range of complex *incompressible* turbulent flows over models based on the conventional eddy-viscosity concept. This experience has encouraged the extension of the models to turbulent flows with strong shock/boundary-layer interaction. Dimitriadis and Leschziner (1990) have implemented an algebraic stress model with the Cell-Vortex scheme. Vandromme *et al.* (1983) and HaMinh *et al.* (1985) solved a complete Reynolds stress model employing the implicit/explicit MacCormack scheme.

While these Reynolds stress models offer a direct extraction of stress quantities without additional approximations, the models are numerically unstable. This is partly due to their highly non-linear and coupled nature and partly due to the lack of turbulent viscosity in the momentum equations as can be found in eddy-viscosity models. As a result, a numerical stabilizing strategy is often required to secure a solution. A major effect in this phase of the study has been focused on these numerical issues.

Calculations based on two variants of the Launder, Reece and Rodi Reynolds-stress model (1975) will be reported: one uses the wall function technique and the other is the low-Reynolds-number extension of Launder and Shima (1989). The former uses the law of the wall to bridge the region between the fully turbulent zone and the wall, while the latter allows a direct integration of all quantities to the wall. While the extension of the low Reynolds number model to compressible flow calculations is straightforward, the use of the wall-function technique requires special attention for the *compressible* law of the wall and the viscous heat generation inside the near-wall layer need to be taken into account.

Results reported in this study are limited only to flow over a flat plate. The Mach number ranges from 2 to 8 for insulated wall; the Mach number is fixed at 5 for

the cold-wall cases, and the wall temperature varies from 20 to 100 percent of the adiabatic wall temperature.

2. Turbulence models

2.1. Reynolds-stress equations

The turbulence model used here is the high-Reynolds-number Reynolds stress model of Launder, Reece and Rodi (1975). The transport equation for $\rho\overline{u_i u_j}$ is

$$\frac{D\rho\overline{u_i u_j}}{Dt} - D_{ij} = P_{ij} + \Phi_{ij} - \rho\epsilon_{ij} \tag{1}$$

The convective and the generation terms, $D\rho\overline{u_i u_j}/Dt$ and

$$P_{ij} = -\rho\left(\overline{u_i u_k}\frac{\partial U_j}{\partial x_k} + \overline{u_j u_k}\frac{\partial U_i}{\partial x_k}\right) \tag{2}$$

are exact and require no approximation. The diffusion term is represented by the generalized gradient diffusion hypothesis;

$$D_{ij} = \frac{\partial}{\partial x_k}\left[\left(c_k\rho\frac{k}{\epsilon}\overline{u_i u_j} + \mu\delta_{kl}\right)\frac{\partial\overline{u_i u_j}}{\partial x_l}\right] \tag{3}$$

The pressure-strain correlation Φ_{ij} is modeled according to Gibson and Launder (1978) to be composed of three processes, namely, Rotta, rapid, and wall-echo terms;

$$\Phi_{ij} = \Phi_{ij,1} + \Phi_{ij,2} + \Phi_{ij,w} \tag{4}$$

In equation (4)

$$\Phi_{ij,1} = -c_1\rho\epsilon a_{ij} \tag{5}$$

$$\Phi_{ij,2} = -c_2\left(P_{ij} - 2/3\delta_{ij}P_k\right) \tag{6}$$

where $P_k = 1/2P_{ii}$ and a_{ij} is the dimensionless anisotropic part of the Reynolds stress,

$$a_{ij} = \frac{\overline{u_i u_j}}{k} - 2/3\delta_{ij} \tag{7}$$

The wall-echo term arises from the reflection of pressure fluctuation from the rigid wall and contains contributions from turbulent and mean strains;

$$\Phi_{ij,w} = \Phi_{w1,ij} + \Phi_{w2,ij} \tag{8}$$

where

$$\Phi_{w1,ij} = c_{1w}\rho\frac{\epsilon}{k}(\overline{u_k u_m}n_k n_m\delta_{ij} - 3/2\overline{u_k u_i}n_k n_j - 3/2\overline{u_k u_j}n_k n_i)f \tag{9}$$

and

$$\Phi_{w2,ij} = c_{2w}\rho\frac{\epsilon}{k}(\Phi_{km,2}n_k n_m\delta_{ij} - 3/2\Phi_{ki,2}n_k n_j - 3/2\Phi_{kj,2}n_k n_i)f \tag{10}$$

The wall damping function, f, is taken as $0.4k^{3/2}/\epsilon y_n$, y_n being the distance normal to the wall. Finally, dissipation is assumed isotropic,

$$\epsilon_{ij} = 2/3\epsilon\delta_{ij} \tag{11}$$

The turbulence energy dissipation rate is governed by solving

$$\frac{D\rho\epsilon}{Dt} = \frac{\partial}{\partial x_k}\left[\left(c_\epsilon\rho\frac{k}{\epsilon}\overline{u_k u_l} + \mu\delta_{kl}\right)\frac{\partial\epsilon}{\partial x_l}\right] + c_{\epsilon 1}\frac{\epsilon}{k}P_k - c_{\epsilon 2}\frac{\rho\epsilon^2}{k} \tag{12}$$

The suggested constants are (Launder and Gibson, 1978):

c_1	c_2	c_{1w}	c_{2w}	c_k	c_ϵ	$c_{\epsilon 1}$	$c_{\epsilon 2}$
1.8	0.6	0.5	0.18	0.22	0.18	1.44	1.92

Launder and Shima (1989) have extended (1) to the viscous sub-layer. The basic ingredient is to introduce three dimensionless parameters to modify the model constants. The dimensionless parameters are the turbulent Reynolds number, $R_t = k^2/\nu\epsilon$, and the second and the third invariants of the stress tensor,

$$II = a_{ij}a_{ji} \tag{13}$$

and

$$III = a_{ik}a_{kj}a_{ji} \tag{14}$$

After systematic tuning, the following modifications to the constants are recommended;

$$c_1 = 1 + 2.58\,A\,II^{1/4}\left[1 - exp\left(-(0.0067R_t)^2\right)\right] \tag{15}$$

$$c_2 = 0.75A^{1/2} \tag{16}$$

$$c_{1w} = -2/3c_1 + 1.67 \tag{17}$$

$$c_{2w} = 2/3(c_2 - 1) + 0.5 \tag{18}$$

$$c_{\epsilon 1} = 1.45 + 2.5A(P_k/\epsilon - 1) + 0.3(1 - 0.3II)exp[-(0.002R_t)^2] \tag{19}$$

$$c_{\epsilon 2} = 1.9 \tag{20}$$

where $A = 1 - 9/8(II - III)$

Furthermore, in order to prevent the sink term of (12) going near to infinity as the wall is approached, the term is modified according to

$$\frac{\epsilon^2}{k} \longrightarrow \frac{\epsilon\,\tilde{\epsilon}}{k} = \frac{\epsilon}{k}\left[\epsilon - 2\nu\left(\frac{\partial k^{1/2}}{\partial y}\right)^2\right] \tag{21}$$

where $\tilde{\epsilon}$ vanishes at the wall.

It should be noted that in the high-Reynolds-number region, the constants provided by Launder and Shima do not revert to those recommended by Launder and Gibson.

2.2. Heat-flux equations

In addition to the stress equations, the heat flux equations are needed in compressible flow calculations. The following assumptions are made to obtain the heat-flux equations:

(1) Following the ASM local-equilibrium assumption, the transport terms are neglected.

(2) The fine scale dissipative motion is assumed to be isotropic, $\Phi_{\overline{u_iT'},w} = 0$.

(3) The wall influence on the pressure-temperature-gradient interaction is assumed insignificant.

The heat-flux equations yield:

$$P_{\overline{u_iT'}} + \Phi_{\overline{u_iT'}} = 0 \tag{22}$$

The generation $P_{\overline{u_iT'}}$ is exact and contains two parts, the stress-temperature-gradient and the heat-flux-strain interactions.

$$P_{\overline{u_iT'}} = P_{\overline{u_iT'},1} + P_{\overline{u_iT'},2} \tag{23}$$

where

$$P_{\overline{u_iT'},1} = -\overline{u_ku_i}\frac{\partial T}{\partial x_k} \tag{24}$$

$$P_{\overline{u_iT'},2} = -\overline{u_kT'}\frac{\partial U_i}{\partial x_k} \tag{25}$$

The pressure-temperature-gradient interaction is modeled to comprise two terms (Launder and Gibson, 1978):

$$\Phi_{\overline{u_iT'}} = \Phi_{\overline{u_iT'},1} + \Phi_{\overline{u_iT'},2} \tag{26}$$

where

$$\Phi_{\overline{u_iT'},1} = -c_{1T}\frac{\epsilon}{k}\overline{u_iT'} \tag{27}$$

$$\Phi_{\overline{u_iT'},2} = -c_{2T}P_{\overline{u_iT'},1} \tag{28}$$

The constants recommended are $c_{T1} = 3$ and $c_{T2} = 0.5$. These constants are used in Reynolds stress calculations employing wall functions.

In the present study, however, it was found that, with $c_{T1} = 3.19$ and $c_{T2} = 0$, the Launder-Shima model provides a better recovery factor for flow over an adiabatic flat plate. This set of constants is thus used for low-Reynolds-number calculations. It is noted that this set of constants is in accord with the one suggested by HaMinh *et al.* (1985).

2.3. Wall functions

The present wall functions follow closely the approach suggested by Bradshaw (1977) and independently by Viegas and Rubesin (1985). For compressible flows, the law of the wall can be expressed as

$$\frac{U_c}{u_\tau} = \frac{1}{\kappa}ln(\frac{u_\tau y}{\nu_w}) + C \tag{29}$$

where U_c is a pseudo-velocity representing the Van-Driest transformation and can be shown to have the following form:

$$\frac{U_c}{u_\tau} = \frac{1}{R}\left\{ sin^{-1}\left[\frac{R(U/u_\tau + H)}{(C_1 + R^2H^2)^{1/2}}\right] - sin^{-1}\left[\frac{RH}{(C_1 + R^2H^2)^{1/2}}\right]\right\} \tag{30}$$

where

$$R = u_\tau\left(\frac{Pr_t}{2c_pT_w}\right)^{1/2} \tag{31}$$

$$H = \frac{q''_w}{\tau_w u_\tau} \tag{32}$$

The constant C and C_1 recommended by Bradshaw (1977) are:

$$C = 5.2 + 95M_t^2 + 30.7B_q + 226B_q^2 \tag{34}$$

$$C_1 = 1 \tag{33}$$

where

$$B_q = \frac{q''_w}{\rho_w c_p u_\tau T_w} \tag{35}$$

$$M_t = \frac{u_\tau}{c_w} \tag{36}$$

c_w and q''_w are the speed of sound and the rate of heat transfer at the wall. The turbulent Prandtl number, Pr_t, is fixed at 0.9 for all calculations.

The heat transfer from the wall to the first finite-volume cell (where $y^+ \approx 30$) is calculated according to:

$$q''_T = q''_w + U_m\tau_w \tag{37}$$

where U_m represents the velocity mid-way between the first grid point and the wall.

The production of Reynolds stresses is modified in the near-wall layer according to

$$-\rho\overline{uv}\frac{\partial U}{\partial y} \approx \frac{1}{y_{cv}}\int_0^{y_{cv}} \tau_w\frac{\partial U}{\partial y}dy \approx \frac{\tau_w U_{cv}}{y_{cv}} \tag{38}$$

where subscript cv indicates the position of control-volume face between the point adjacent to the wall and the one above it.

The average ϵ over the near-wall cell is approximated as:

$$\overline{\epsilon} \approx \frac{\rho c_\mu^{3/4} k^{3/2} U_{cv}^+}{y_{cv}} \tag{39}$$

Finally ϵ at the point adjacent to the wall, 2, is prescribed as;

$$\epsilon_2 = \frac{k_2^{3/2} c_\mu^{3/4}}{\kappa y_2} \tag{40}$$

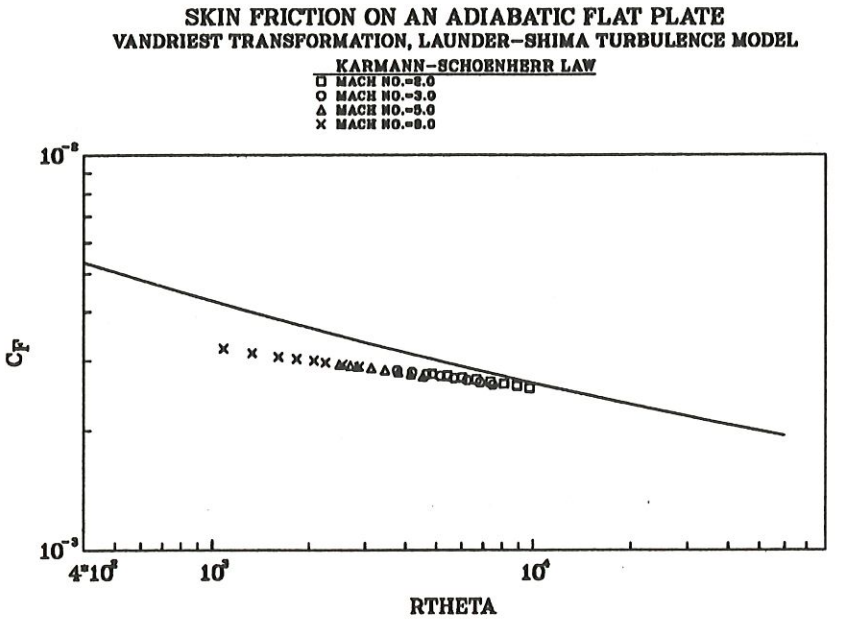

(a)

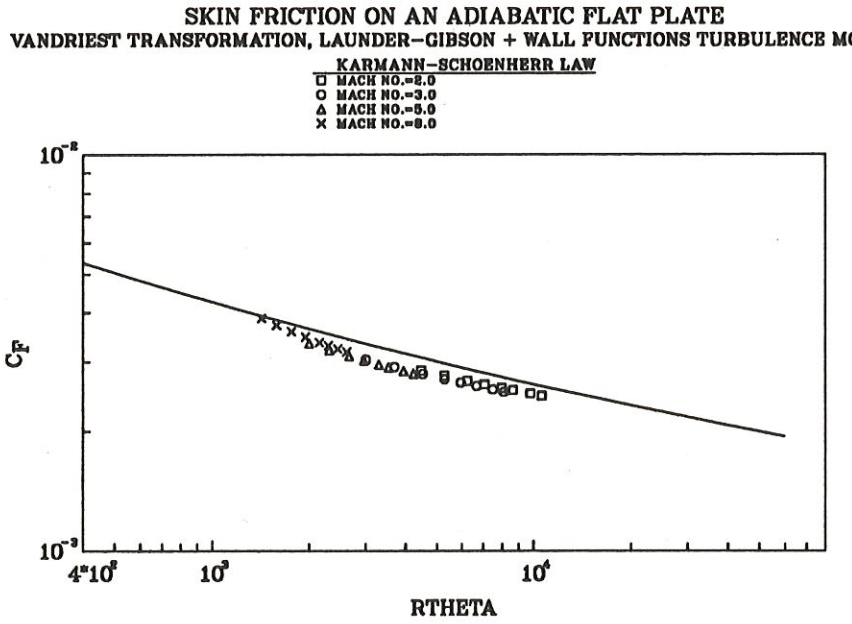

(b)

FIGURE 1. Generalization of adiabatic-wall skin friction, C_f vs. Re_θ, *(a)* L-S, *(b)* L-G.

3. Numerical method

Although the differential equations are expressed in Cartesian coordinates, the code implemented solves the complete 2-D Navier-Stokes' equations in non-orthogonal curvilinear mesh, plane and axisymmetric geometries. All dependent variables are stored at the center of the control-volume cell and a finite-volume principle is applied to impose conservation across the control-volume faces.

TVD schemes are used to discretize the convective terms (Huang, 1989) while the center differencing scheme is used for the diffusive terms. The numerical diffusion provided by the TVD schemes can, on the one hand, prevent unrealistic oscillation in regions where gradient of the dependent variable is high, and on the other hand, offer an "optimum" artificial diffusion to stabilize the calculation.

The numerical algorithm is implicit and is based on a symmetric Gauss-Seidel line-by-line relaxation method, which combines features derived from Gnoffo (1986) and MacCormack (1985). This method, coupled with implicit treatments of the boundary conditions, has been found to provide a rapid acceleration of solution, for it allows a large value of Courant number to be used in the calculation.

4. Accomplishments

Attention is confined in this section to computations of flow over a flat plate: insulated-wall and cooled-wall cases.† Comparisons are made with the Van Driest II theory, which has been found to provide good agreements with the available experimental data (Hopkins and Inouye, 1971).

Figures 1(a) and 1(b) show variations of the adiabatic-wall skin friction with Re_θ, obtained from the Launder-Shima model (L-S) and the Launder-Gibson-wall-function model (L-G), respectively. The Van Driest II theory is used to deduce the incompressible results from the compressible calculations. The solid line is the Kármán-Schoenherr formula, and the symbols represent results obtained from calculations. The results have shown that L-S returns an incorrect slope of the skin friction variation, reflecting a poor prediction of the skin friction at high Mach number, shown in Figure 2(a). In contrast, L-G results in a correct slope of the skin friction variation while the predicted values are slightly lower than the experimental correlation, as depicted in Figure 2(b).

The skin friction profiles on a non-adiabatic plate at Mach number equal to 5 are shown in Figure 3. Again, the Van Driest II formula is used to scale all predicted data to the incompressible one. For calculations based on T_w equal to adiabatic wall temperature, T_{aw}, both L-S and L-G return results similar to those shown in Figure 1.

As shown in Figure 3(a), L-S still displays the same incorrect slope of skin friction profile, resulting in a better skin friction prediction at low T_w. While Figure 4(a) shows that L-S provides a good prediction for $T_w/T_{aw} = 0.2$, it should be noted that the experimental data does not seem to support the Van Driest II theory for region where $T_w/T_{aw} < 0.3$. The failure of L-S can also be depicted in Figure 5(a)

† Some of these results are presented in a recent paper by Coakley *et al.* (1990)

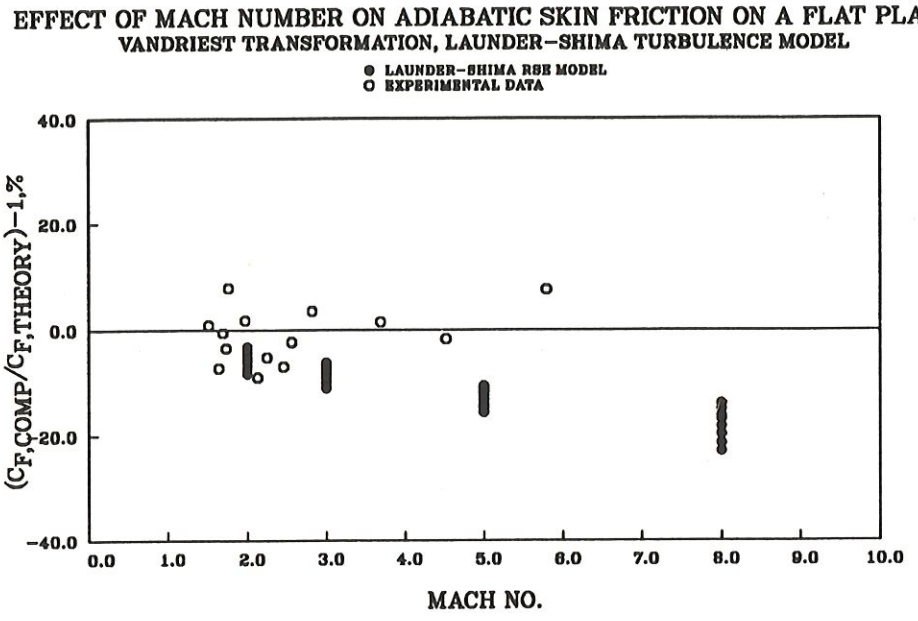

(a)

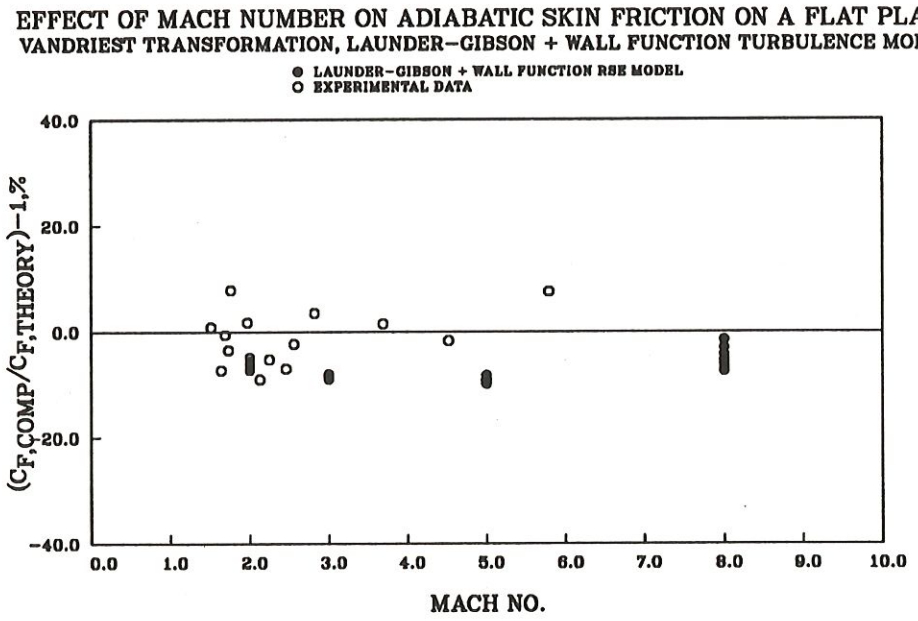

(b)

FIGURE 2. Effect of Mach number on adiabatic-wall skin friction, *(a)* L-S, *(b)* L-G.

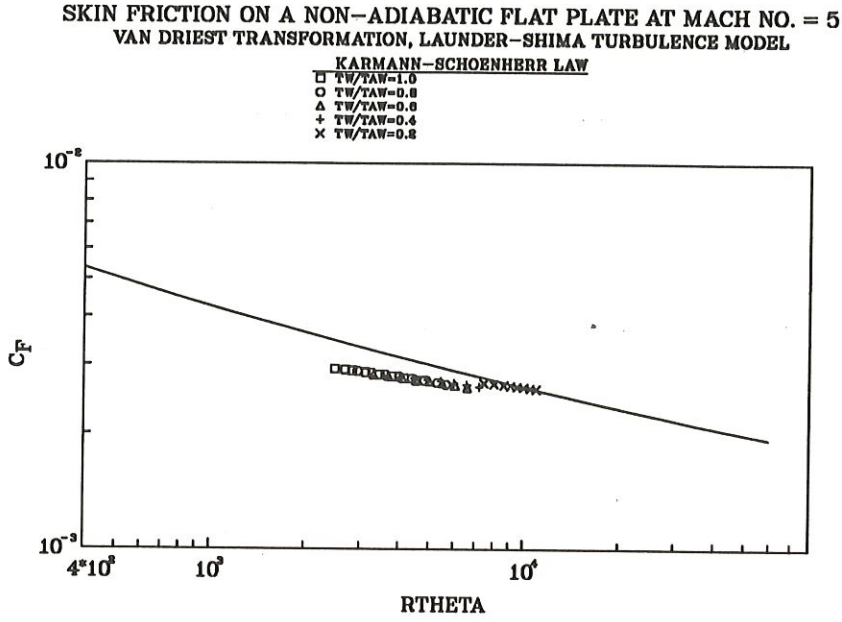

(a)

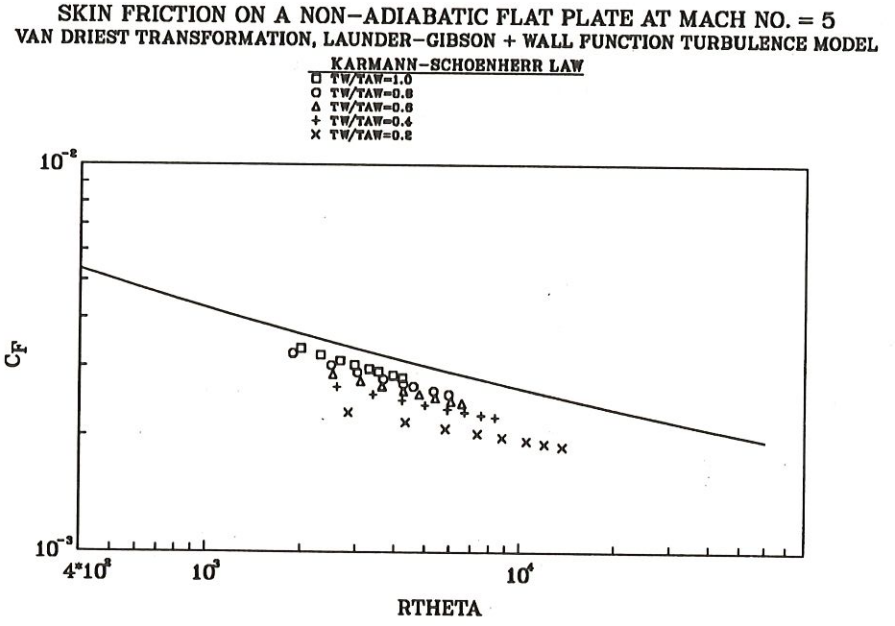

(b)

FIGURE 3. Generalization of non-adiabatic-wall skin friction, C_f vs. Re_θ, *(a)* L-S, *(b)* L-G.

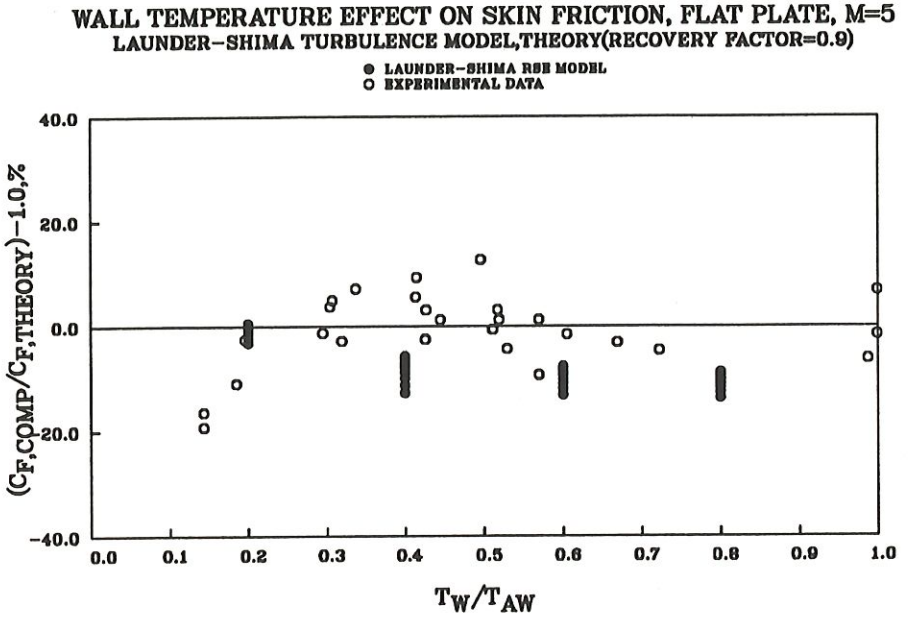

(a)

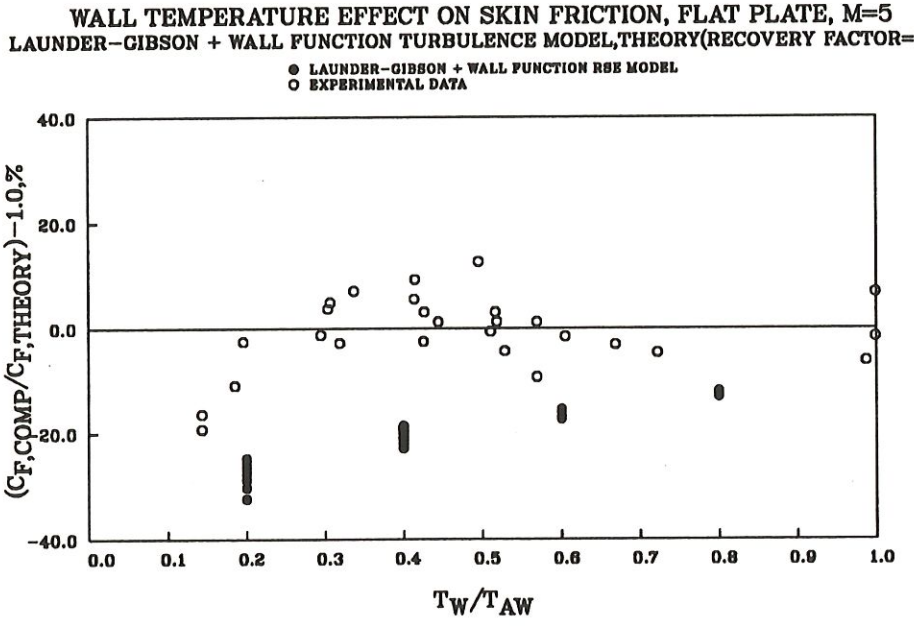

(b)

FIGURE 4. Wall temperature effect on skin friction at $M = 5$, *(a)* L-S, *(b)* L-G.

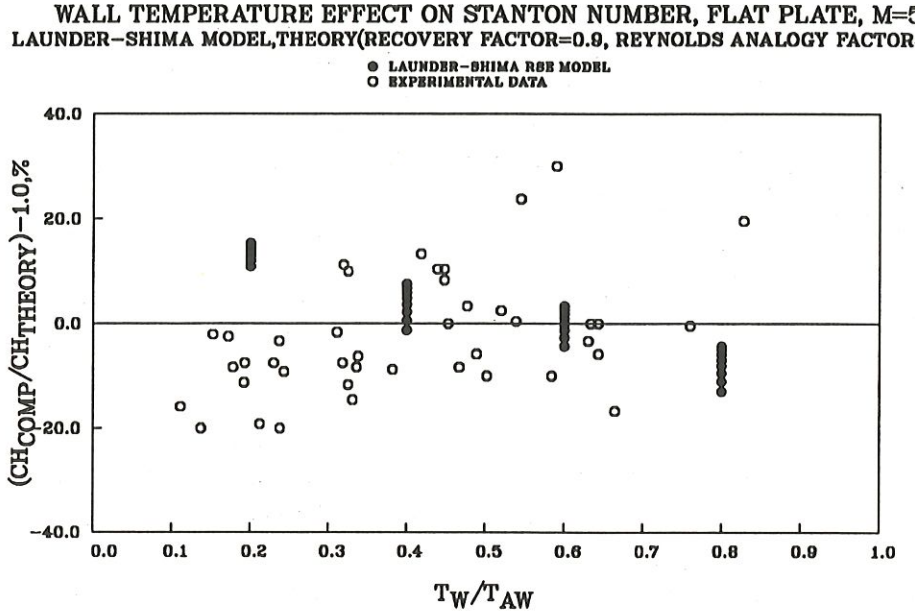

(a)

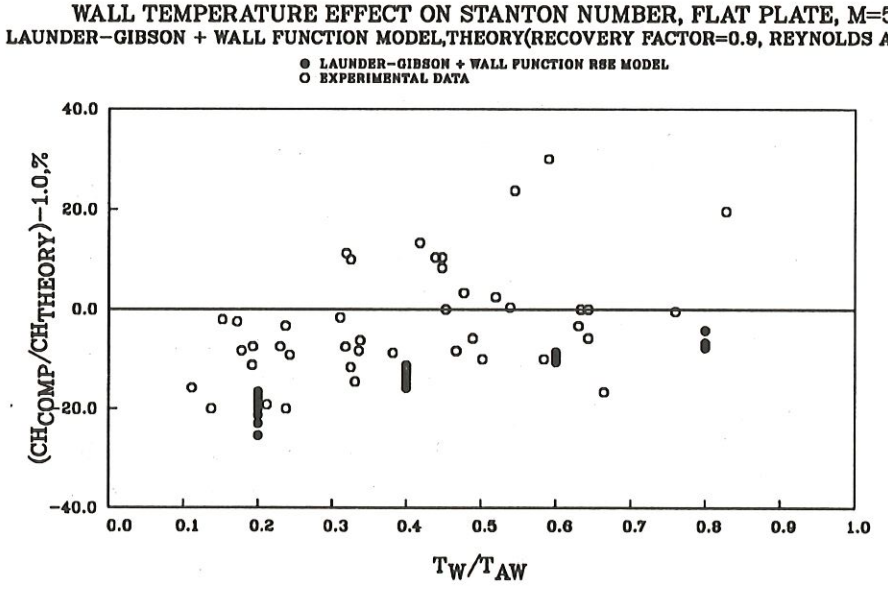

(b)

FIGURE 5. Wall temperature effect on Stanton number at $M = 5$, *(a)* L-S, *(b)* L-G.

where Stanton number are compared in a manner analogous to the skin friction shown in Figure 4(a). The theoretical Stanton number, $(C_h)_{the}$, is obtained by assuming a recovery factor of 0.9 and a Reynolds analog factor of 1.0. It can be found that Stanton number prediction does not agree well with the experimental data. The experimental data shows a positive slope across the theoretical line while the prediction displays a negative slope.

In contrast, L-G tends to under-predict the skin friction and the Stanton number at low wall temperature, showing a departure of the predicted values away from the theoretical ones as the wall temperature decreases. This observation has suggested that improvements of the wall functions for non-adiabatic flows are needed.

5. Future plans

(1) Improve the Launder-Shima model for high Mach number flow.

(2) Consider the FRAME model (HaMinh *et al.*, 1985), which has been found to offer excellent agreements in predicting the above-mentioned flow (Coakley *et al.*, 1990).

(3) Modify the wall functions to predict flow in non-adiabatic conditions.

(4) Extend the Reynolds Stress models to complex hypersonic flows.

REFERENCES

BRADSHAW, P. 1977 Compressible turbulent shear layers. *Ann. Rev. Fluid Mech.* **9**, 33-54.

COAKLEY, T. J., VIEGAS, J. R., HUANG, P. G. & RUBESIN, M. W. 1990 An assessment and application of turbulence models for hypersonic flows. 9th National Aero-Space Plane Technology Sym.. **106**, Orlando, Florida.

DIMITRIADIS, K. P.& LESCHZINER, M. A. 1990 Modeling shock/turbulent-boundary-layer interaction with a cell-vortex scheme and second-moment closure. 12th Int. Conf. on Num. Meths. in Fluid Dynamics, Oxford, England.

GIBSON, M. M.& LAUNDER, B. E. 1978 Ground effects on pressure fluctuation in the atmospheric boundary layer. *J. Fluid Mech.* **86**, 491-511.

GNOFFO, P. A. 1986 Application of program Laura to three dimensional AOTV flow fields. *AIAA-86-0565.* 24th Aerospace Sciences Meeting, Reno, NV.

HAMINH H., RUBESIN, M.W., VANDROMME, D. & VIEGAS, J. R. 1985 On the use of second order closure modeling for the prediction of turbulence boundary layer/shock wave interaction: physical and numerical aspects. Int. Sym. on Computational Fluid Dynamics, Tokyo, Japan.

HOPKINS, E.& INOUYE, M. 1971 An evaluation of theories for predicting turbulent skin friction and heat transfer on flat plates at supersonic and hypersonic Mach numbers. *AIAA J.* **9**, 6, 993-1003.

HUANG, P. G. 1989 A numerical method for prediction of compressible turbulent flows with closure models. *Annual Research Briefs - 1989.* Center for Turbulence Research, 185-193.

LAUNDER, B. E., REECE, G. J. & RODI, W. 1975 Progress in the development of a Reynolds-stress turbulence closure. *J. Fluid Mech.* **68**, 537-566.

LAUNDER, B. E. & SHIMA, N. 1989 Second-moment closure for the near-wall sublayer: development and application. *AIAA J.* **27**, 10, 1319-1325.

MACCORMACK, R. W. 1985 Current status of numerical solutions of the Navier-Stokes equations. *AIAA-85-0032.* 23rd Aerospace Sciences Meeting, Reno, NV

VANDROMME, D., HAMINH, H., VIEGAS, J. R., RUBESIN, M. W. & KOLLMANN, W. 1983 Second order closure for the calculation of compressible wall bounded flows with an implicit Navier-Stokes solver. 4th Sym. on Turbulent Shear Flows, Karlsruhe, Germany.

VIEGAS, J. R. & RUBESIN, M. W. 1985 On the use of wall-functions as boundary conditions for two-dimensional separated compressible flows. *AIAA-85-0180.* 23rd Aerospace Sciences Meeting, Reno, NV.